SLAC-PUB-655
December 1969
(TH) and (EXP)

REGGE ANALYSIS OF π^{o} AND π^{+} PHOTOPRODUCTION AT BACKWARD ANGLES*

J. V. Beaupre† and E. A. Paschos††

Stanford Linear Accelerator Center
Stanford University, Stanford, California 94305

ABSTRACT

By correlating recent experimental results on π^{o} and π^{+} photoproduction at backward angles with results on $\pi^{-}p \rightarrow p p^{-}$ at the same angles, it is found that any explanation of the three processes in terms of Regge poles must involve at least two isospin 1/2 trajectories. Furthermore the two trajectories must be almost degenerate. Such a solution makes definite predictions about other processes which can be checked by experiments.

(Submitted to Phys. Rev.)

---

* Work supported by the U.S. Atomic Energy Commission

† A.E.C. Postdoctoral Fellow. Aachen Technischen Hochschule, Aachen, Germany.

†† Present address: Rockefeller University, New York, New York.

INTRODUCTION

The first data[1] on the photoproduction of π^+ mesons at backward angles imposed restrictions on the contribution of various trajectories.[2] These restrictions become more limiting now that there are accurate data[3-5] available for the processes $\gamma p \to p\pi^+$, $\gamma p \to p\pi^o$ and $\pi^- p \to p\rho^-$. In fact by correlating these processes one arrives at the conclusion that an analysis of the data in terms of traditional Regge poles is non-trivial and it requires the contribution of at least three trajectories. Furthermore, the contribution of the $I = 3/2$ trajectories to photoproduction has an upper bound and the $I = 1/2$ trajectories must be almost degenerate.

In view of the above results we feel it is justified to neglect for the moment the contribution of the absorption cuts,[6] which has not yet been formulated completely, and deal with a three pole model which leads to definite conclusions. These conclusions can easily be checked experimentally. In case that they are violated we feel that a simple pole model is inadequate and impractical and that the contribution of cuts is essential.

In the next section we give the basic Regge formalism and relate the residues to the coupling constants of the Born diagrams determined in the isobar model.[7] In Section III, we summarize the experimental situation that requires us to introduce the N_γ-trajectory, we obtain from vector meson dominance an upper bound for the contribution of the $I = 3/2$ trajectories to photoproduction and give the parametrization of the amplitudes. The last section discusses the main results of the model and proposes experimental checks.

II. FORMALISM

The kinematics of photoproduction have been discussed in several places. We adopt the C.G.L.N. notation.[8] The C.G.L.N. amplitudes have kinematic singularities, which become apparent when one writes them in terms of the J. Ball[9] amplitudes which satisfy the Mandelstam representation:

$$\mathscr{F}_1(W) = \frac{W-M}{8\pi W}(E_1+M)^{1/2}(E_2+M)^{1/2}\left[B_1 - \frac{1}{2}(W+M)B_4 + \frac{t-\mu^2}{2(W-M)}B_3 - \frac{1}{2}B_4\right] \qquad \text{(II.1a)}$$

$$\mathscr{F}_2(W) = \frac{W-M}{8\pi W}\, q\left(\frac{E_1+M}{E_2+M}\right)^{1/2}\left[-B_1 - \frac{1}{2}(W-M)B_4 + \frac{t-\mu^2}{2(W+M)}B_3 - \frac{1}{2}B_4\right] \qquad \text{(II.1b)}$$

$$\mathscr{F}_3(W) = \frac{W-M}{8\pi W}\, q(E_1+M)^{1/2}(E_2+M)^{1/2}\left[\frac{2(W-M)}{t-\mu^2}B_2 - B_3 + \frac{1}{2}B_4\right] \qquad \text{(II.1c)}$$

$$\mathscr{F}_4(W) = \frac{W-M}{8\pi W}\, q^2\left(\frac{E_1+M}{E_2+M}\right)^{1/2}\left[-\frac{2(W+M)}{t-\mu^2}B_2 - B_3 + \frac{1}{2}B_4\right] \qquad \text{(II.1d)}$$

where

$$W = \sqrt{u}\,, \qquad k = (u-M^2)/2W$$

$$E_1 \pm M = (W\pm M)^2/2W, \qquad E_2 \pm M = \left[(W\pm M)^2 - \mu^2\right]/2W$$

$$q = \left[(W+M)^2 - \mu^2\right]^{1/2}\left[(W-M)^2 - \mu^2\right]^{1/2}/2W$$

The cosine of the u channel scattering angle is given by:

$$z_u = \cos\theta_u = -\frac{2su - 2M^2u + (u-M^2)(u+M^2-\mu^2)}{(u-M^2)\left[u-(M+\mu)^2\right]^{1/2}\left[u-(M-\mu)^2\right]^{1/2}} \qquad \text{(II.2)}$$

The phase conventions for the several square roots appearing above are these: All expressions of the form $(W-a)^{1/2}$ have a branch point at W=a and the cut lies along the negative real (W-a) axis. Slightly above the cut the phase of $(W-a)^{1/2}$ is $\pi/2$. Products like $(W^2-a^2)^{1/2}$ have cuts between +a and -a, and they satisfy:

$$(W-a)^{1/2} \xrightarrow[|W| \to \infty]{} W$$

Thus in the backward direction (z_s=-1) one has z_u=-1, and at u=0, z_u=+1. The fact that z_u is not large for backward angles is not very alarming since a sequence of daughter trajectories can restore the Regge asymptotic behavior.

A. McDowell Symmetry

Since the $B_i(s,u)$ are even functions of W, we can derive relations between $\mathscr{F}_i(W)$ and $\mathscr{F}_i(-W)$. With the phase convention adopted in the previous section we obtain:

$$\mathscr{F}_1(W) = \mathscr{F}_2(-W) \qquad \text{(II.3a)}$$

$$\mathscr{F}_3(W) = \mathscr{F}_4(-W) \qquad \text{(II.3b)}$$

B. Singularities at u=0

Since the line u=0 is within the physical region, special care must be taken so that the combinations of sines and cosines of $\theta_u/2$ together with the linear combinations of the $\mathscr{F}_i(W)$ which appear in the helicity amplitudes are smooth around the line u=0. Assuming that the B_i amplitudes approach constants as $W \to 0$, we find that the most singular behavior of the sums and differences is given by

$$\mathscr{F}_1(W) + \mathscr{F}_2(W) \longrightarrow C_1/W^2 \qquad \text{(II.4a)}$$

$$\mathscr{F}_1(W) - \mathscr{F}_2(W) \longrightarrow C_2/W \tag{II.4b}$$

$$\mathscr{F}_3(W) + \mathscr{F}_4(W) \longrightarrow C_3/W^2 \tag{II.4c}$$

$$\mathscr{F}_4(W) - \mathscr{F}_4(W) \longrightarrow C_4/W^3 \tag{II.4d}$$

The trigonometric functions of $\theta_u/2$ behave as

$$\sin \theta_u/2 \propto W$$

$$\cos \theta_u/2 \longrightarrow 1 \quad .$$

Therefore the following u-channel helicity amplitudes vary smoothly over the line u=0;

$$A_{1/2,\,3/2} = -\sqrt{2}\,\pi W\,(\mathscr{F}_3 + \mathscr{F}_4)\,\sin\theta_u \cos\tfrac{1}{2}\theta_u \tag{II.5a}$$

$$A_{1/2,\,1/2} = \sqrt{2}\,\pi W\left(2\left[\mathscr{F}_2 - \mathscr{F}_1\right]\cos\tfrac{1}{2}\theta_u + \left[\mathscr{F}_3 - \mathscr{F}_4\right]\sin\theta_u \sin\tfrac{1}{2}\theta_u\right) \tag{II.5b}$$

$$A_{-1/2,3/2} = \sqrt{2}\,\pi W\,(\mathscr{F}_3 - \mathscr{F}_4)\,\sin\theta_u \sin\tfrac{1}{2}\theta_u \tag{II.5c}$$

$$A_{-1/2,1/2} = \sqrt{2}\,\pi W\left(2\left[\mathscr{F}_2 + \mathscr{F}_1\right]\sin\tfrac{1}{2}\theta_u + \left[\mathscr{F}_3 + \mathscr{F}_4\right]\sin\theta_u \cos\tfrac{1}{2}\theta_u\right) \tag{II.5d}$$

C. Normalization

The differential cross section is given by

$$\frac{d\sigma}{du} = \frac{1}{4\pi s k_s^2}\sum_{\lambda\mu} |A_{\lambda\mu}|^2 \tag{II.6}$$

where k_s is the center-of-mass momentum in the s channel, and $A_{\lambda\mu}$ the u channel amplitudes, $\lambda(\mu)$ being the final (initial) center-of-mass helicity.

At 180^o, where $z_s = z_u = -1$, only the $A_{-(1/2,\,1/2)}$ amplitudes is non-vanishing. In case that the contribution of the other amplitudes is non-negligible we expect a minimum at 180^o.

D. Reggeization

The Reggeization of the amplitudes incorporates all of the above properties. Because of the McDowell symmetry, we Reggeize only $\mathscr{F}_2$ and $\mathscr{F}_4$; $\mathscr{F}_1$ and $\mathscr{F}_3$ are obtained by reflection in W. In terms of the electric and magnetic multipoles, $M_{\ell\pm}(W)$ and $E_{\ell\pm}(W)$, with $j = \ell \pm \frac{1}{2}$, the partial wave expansions are given by:

$$\mathscr{F}_2(W) = \sum_{\ell=1} \left[(\ell+1)\, M_{\ell+}(W) + M_{\ell-}(W)\right] P'_\ell(z_u) \tag{II. 7a}$$

$$\mathscr{F}_4(W) = \sum_{\ell=1} \left[M_{\ell+}(W) - E_{\ell+}(W) - M_{\ell-}(W) - E_{\ell-}(W)\right] P''_\ell(z_u) \tag{II. 7b}$$

The combinations $\ell M_{\ell-}$, $\ell E_{\ell-}$, $(\ell+1)E_{\ell+}$, $(\ell+1)M_{\ell+}$ can have dynamic poles in the complex j plane. For a given Regge pole at $j = \alpha$, the leading contributions come from $M_{\ell-}$ and $E_{\ell-}$. Thus we keep only the $\ell M_{\ell-}$ in $\mathscr{F}_2$. Assuming

$$M_{\ell-}(W) = \frac{\beta_2(W)}{j - \alpha} \tag{II. 8}$$

we obtain the Reggeization:

$$\mathscr{F}_2(W) = \sqrt{\pi}\, \beta_2(W) \frac{1 + \eta\, e^{-i\pi(\alpha - 1/2)}}{\sin \pi\left(\alpha - \frac{1}{2}\right) \Gamma\left(\alpha + \frac{1}{2}\right)} \left(\frac{s}{kq}\right)^{\alpha - 1/2} \tag{II. 9}$$

For $\mathscr{F}_4$ we assume

$$E_{\ell-}(W) + M_{\ell-}(W) = \frac{\beta_4(W)}{j - \alpha} \tag{II. 10}$$

and obtain:

$$\mathscr{F}_4(W) = -2\sqrt{\pi}\, \beta_4(W) \frac{1 + \eta\, e^{-i\pi(\alpha - 1/2)}}{\sin \pi\left(\alpha - \frac{1}{2}\right) \Gamma\left(\alpha - \frac{1}{2}\right)} \left(\frac{s}{kq}\right)^{\alpha - 3/2} \tag{II. 11}$$

Introducing the scaling parameter s_0 and extracting the kinematic singularities, we obtain a set of residues $\gamma_i(W)$ which contain only dynamic information:

$$\beta_2(W) = \left[(W-M)^2 - \mu^2\right]^{1/2} (1-M^2/u)(kq/s_0)^{\alpha-1/2}\ \gamma_2(W) \tag{II.12a}$$

$$\beta_4(W) = \frac{1}{2} q \left[(W-M)^2 - \mu^2\right]^{1/2} (1-M^2/u)(kq/s_0)^{\alpha-3/2}\ \gamma_4(W) \tag{II.12b}$$

The resulting form of the Reggeized amplitudes are

$$\mathscr{F}_2(W) = \frac{u-M^2}{\sqrt{\pi u}} \left[(W-M)^2 - u^2\right]^{1/2} \sum_\alpha \gamma_2^\alpha \left(1+\eta e^{-i\pi(\alpha-1/2)}\right) \Gamma(1/2-\alpha)(s/s_0)^{\alpha-1/2} \tag{II.13a}$$

$$\mathscr{F}_4(W) = \frac{u-M^2}{\sqrt{\pi u}} q \left[(W-M)^2 - u^2\right]^{1/2} \sum_\alpha \gamma_4^\alpha \left(1+\eta e^{-i\pi(\alpha-1/2)}\right) \Gamma(3/2-\alpha)(s/s_0)^{\alpha-3/2} \tag{II.13b}$$

E. Born Diagrams

We evaluate the residues of the three leading trajectories at the poles by using Born diagrams. The nucleon residue at the pole is obtained by using Feynman rules and then using Eqs. (II.8) and (II.12a) to obtain

$$\gamma_2^E(N_\alpha, W) = \frac{eG}{32\pi} \frac{d\alpha}{du} \tag{II.14a}$$

$$\gamma_2^M(N_\alpha, W) = \frac{\mu_i G}{32\pi} (W+M) \frac{d\alpha}{du} \tag{II.14b}$$

where

$$G^2/4\pi = 14.5\ , \qquad e^2/4\pi = 1/137\ ,$$

$$\mu_p = 1.78\ e/2M\ , \text{ and } \qquad \mu_n = -1.91\ e/2M\ .$$

In estimating the residues of the $N\gamma$ and the Δ trajectories we use the isobar model of Gourdin and Salin.[7] The contribution of the $N\gamma$ resonance to the $M_{2-}(W)$

partial wave is

$$M_{2-}(W) = \frac{1}{6} L_2 \frac{\left[(E_1 + M)(E_2 + M)\right]^{1/2}}{8\pi W} \tag{II.15}$$

where

$$L_2 = .1 \left(\frac{e}{\sqrt{4\pi}}\right)\left(\frac{G}{\sqrt{4\pi}}\right) 4\pi \tag{II.16}$$

In (II.15) we have corrected for the normalization differences between references 7 and 8, but we have not included any isotopic spin factors. Using (II.15), (II.8) and (II.12a) we can obtain $\gamma_2(N\gamma)$. In a similar way we can estimate the Δ-residue. The numerical results using the coupling constants of Gourdin and Salin[7] are:

$$\frac{\gamma_2(N_\alpha)}{\gamma_2(N\gamma)} \approx 1.0 \qquad \text{and} \qquad \frac{\gamma_2(N\gamma)}{\gamma_2(\Delta)} \approx .1$$

III. EXPERIMENTAL SUMMARY AND PARAMETERIZATION

The π^+ and π^o photoproduction data[3,4] can be combined in such a way that one can make rather strong arguments about the contributions of the allowed baryon exchanges. On the other hand, application of vector meson dominance imposes additional constraints on the contributions of the trajectories. There are three rather important features of the data and we discuss them in detail:

1. The traditional nucleon trajectory has a nonsense zero at $u \simeq -.15\,(\text{BeV/c})^2$, which appears in all four helicity amplitudes. The absence of a dip in this u region in both the π^o and π^+ photoproduction eliminates the dominance of the N_α trajectory. Presumably this argument is weakened if the nucleon contribution is composed of the usual Regge contribution and an N_α-Pomeron cut;[6] or if there is a fixed pole in the N_α residues at $\alpha(N_\alpha) = -1/2$. Since the understanding of cuts and fixed poles is rather limited, we restrict our discussion to conventional Regge poles.

2. If one makes a conventional Regge model containing only the N_α and the Δ poles, only the Δ contribution survives at the position the nucleon zero. Since the pure $\Delta(I=3/2)$ contribution involves only the isovector part of the photon, the vanishing of the I=1/2 contribution(s) imply

$$\left(\frac{d\sigma}{du}\right)_{\gamma p \to p\pi^o} = 2\left(\frac{d\sigma}{du}\right)_{\gamma p \to n\pi^+} \tag{III.1}$$

The recent experimental data show that these two cross sections are equal for $-.3 < u < 0.0$. Therefore there must exist a non-vanishing I=1/2 contribution at $u \simeq -.15$. Since we are forced to consider another I=1/2 trajectory, we may ask whether the $\Delta(I=3/2)$ contribution is completely negligible. The present data are consistent with an I=1/2 contribution alone, since one can vary the isoscalar and isovector ratios as a function of u to account for the observed cross sections.

3. The above argument does <u>not</u>, however, eliminate the I=3/2 exchange contributions. Assuming vector meson dominance, there is an experimental way to estimate the I=3/2 contribution to $\gamma p \to n\pi^+$ and $\gamma p \to p\pi^o$. This method relates the photoproduction contributions to the pure Δ exchange process $\pi^- p \to p\rho^-$, by

$$\left[\Delta \text{ contribution to } \frac{d}{du}(\pi^- p \to n\rho^o)\right] = 2/9\,\frac{d\sigma}{du}(\pi^- p \to p\rho^-) \tag{III.2a}$$

$$\left[\Delta \text{ contribution to } \frac{d}{du}(\gamma p - n\pi^+)\right] = \frac{1}{4}\,\frac{e^2}{\gamma_\rho^2}\left(\frac{p_\pi}{p_\rho}\right)^2 \rho_{11}(u)$$
$$\times\left[\Delta \text{ contribution to } \frac{d\sigma}{du}(\pi^- p \to n\rho^o)\right] \tag{III.2b}$$

Accurate knowledge of the helicity density matrix element $\rho_{11}(u)$ and of the γ-ρ coupling constant together with the $\pi^- p \to p\rho^-$ data[5] can determine accurately the Δ contribution alone to photoproduction cross sections. The knowledge of $\rho_{11}(u)$ is rather limited, but one can still obtain an upper bound on the Δ contribution.

Table 1 shows the upper bounds for π^+ and π^o photoproduction obtained for $\rho_{11}(u) = 1/2$, $\gamma_\rho^2/4\pi = 1/2$. Comparison of the upper bounds and the experimental photoproduction cross sections show that the I=3/2 trajectories could be a significant part of the photoproduction cross sections. In particular, Δ exchange could account for most of the π^o photoproduction cross section and about $\frac{1}{4} \simeq \frac{1}{2}$ of the π^+ cross sections.

In summary, the arguments 1 to 3 imply that an I=1/2 contribution, different from the traditional nucleon, is needed. Argument 3 does not imply that the Δ is necessarily negligible as was emphasized by G. Kane.[10]

We therefore use not only the N_α and Δ trajectories but also the $N\gamma$ trajectory in our parametrization of the amplitudes. The $N\gamma$ trajectory is the needed I=1/2 exchange suggested by arguments 1 to 3 and by the isobar model, previously discussed.

The trajectories are obtained as follows:

The N_α and Δ trajectories are taken from previous parametrizations of Refs. 11 and 12, to the reactions $\pi^+ p \longrightarrow p\pi^+$, $\pi^- p \longrightarrow p\pi^-$ and $\pi^- p \longrightarrow p\rho^-$.

The nucleon trajectory that we use is:

$$\alpha = -0.34 + 0.093\,W + 1.15\,W^2 \qquad \text{(III.3)}$$

taken from the work of Chiu and Stack.[11] For the Δ trajectory, we added a term linear in W to Shih's determination,[12] so that the trajectory passes through the (1238) mass, to obtain:

$$\alpha = 0.05 + 0.25\,W + 0.75\,W^2 \qquad \text{(III.4)}$$

The $N\gamma$ trajectory is constrained to pass through the first two N resonances ($N\gamma(1520)\ 3/2^-$, $N\gamma(2190)\ 7/2^-$) and also contains a term linear in W. The trajectory intercept was chosen as a free parameter:

$$\alpha = x - (0.385 + 1.105\,x)\,W + (0.88 + 0.278\,x)\,W^2 \qquad \text{(III.5)}$$

The residues $\gamma_i^{\alpha}(W)$ have the following form:

$$\gamma_2 = I_\alpha a_\alpha (1 + b_\alpha W) \tag{III.6a}$$

$$\gamma_4 = I_\alpha c_\alpha (1 + d_\alpha W)\, e^{hu} \tag{III.6b}$$

where I_α is an isospin factor which depends on the coupling of the various trajectories to the u channel vertices, and is given in Table 2. The parameter S/V (see Table 2) occurs for the nucleon trajectories because the nucleons can couple to both the isovector and isoscalar components of the photon. We take this ratio to be a constant and the same for all residues and I=1/2 trajectories.

As can be seen in Figs. 1 and 2, we obtained an excellent fit to the photoproduction data. The chi-square was found to be 92.5 for 60 degrees of freedom. The quality of the fit did not change appreciably when a different nucleon trajectory,[13]

$$\alpha = -0.38 + 0.91\, W^2 \tag{III.7}$$

was substituted for the one given in Eq. (III.3).

The rest of the parameters are given by:

N_α:	$a = -1.41 \times 10^{-3}/\text{BeV}^2$,	$b = 8.43/\text{BeV}$,
	$c = 1.10 \times 10^{-2}/\text{BeV}^3$,	$d = -22.9/\text{BeV}$.
Δ:	$a = -3.66 \times 10^{-3}/\text{BeV}^2$,	$b = 7.78/\text{BeV}$,
	$c = 5.25 \times 10^{-2}/\text{BeV}^3$,	$d = 1.97/\text{BeV}$.
$N\gamma$:	$a = 6.45 \times 10^{-2}/\text{BeV}^2$,	$b = 0.031/\text{BeV}$,
	$c = -8.20 \times 10^{-2}/\text{BeV}^3$,	$d = -0.778/\text{BeV}$.

$s_0 = 3.83\ \text{BeV}^2$

$S/V = -0.376$

$h = 4.19/\text{BeV}^2$

$x = \alpha(N\gamma, 0) = -0.546$

giving the $N\gamma$ trajectory:

$$\alpha = -0.546 + 0.22\, W + 0.73\, W^2 .$$

IV. CONCLUSIONS AND EXPERIMENTAL CHECKS

An interpretation of the data in terms of three trajectories demands a delicate balance among them. In fact, this analysis relies heavily on the degeneracy between the N_α and $N\gamma$ trajectories, as well as the dominance of the Δ trajectory in some regions. We summarize below those conclusions of the model that can be checked experimentally.

A. N_α-$N\gamma$ Degeneracy

In the region $-1 \lesssim u \lesssim 0.0$, the N_α and $N\gamma$ trajectories are almost degenerate. Such a degeneracy has already been proposed in the literature:

1. Several theoretical models predict an N_α-$N\gamma$ exchange degeneracy.[14]
2. Both the absence of resonances in the pp system and the absence of the N_α dip in $pp \to D\pi^+$ can be explained in terms of degenerate N_α and $N\gamma$ trajectories.[15] This degeneracy can be checked at places where the Δ contribution is small by comparing $\gamma p \to n\pi^+$ to the crossing symmetric process $\bar{p}n \to \pi^- \gamma$. Furthermore a better check of the exchange degeneracy can be obtained by comparing the crossing symmetric processes $pp \to D\pi^+$ and $\pi^- p \to \bar{p}D$.[15]

B. The Δ Contribution

We find that the delta contribution is large and in some places dominant. The percentages of the I=1/2 and delta contributions to π^+ production at photon energies of 4 and 20 BeV are shown in Fig. 3. The upper bounds of the delta contribution, given in Table 1, are exceeded by our model for $|u| \gtrsim .3\ \mathrm{BeV}^2$, for the π^+ data, and most of the π^0 data. In the large u region where the $N\gamma$ has a wrong signature minimum the delta trajectory is dominant. It would be very interesting to extend the $\pi^- p \rightarrow p\rho^-$ data to this region to determine whether or not the delta contribution of the model drastically violates the upper bounds. A large violation for a simple Regge model would imply that the role of cuts is very important and can not be ignored in photoproduction.

Another motivation for extending the $\pi^- p \longrightarrow p\rho^-$ data to larger values of $|u|$ comes from the following observation. When we separate the isovector contribution of the photon, by setting S/V equal to zero in our solution, we can relate it to $\rho_{11}\, d\sigma/du(\pi^- p \longrightarrow n\rho^0)$ using the vector meson dominance model. Such a comparison has been done by Z. G. T. Guiragossián[16] who concludes that the agreement is satisfactory at $E_{LAB} = 4$ BeV and $-1.0 \lesssim u < 0.0$, but it is not very satisfactory in the larger $|u|$ region.

C. Photoproduction of π^- at Backward Angles

The $\gamma n \longrightarrow p\pi^-$ cross section can be predicted within this model. Figure 4 gives the calculated cross section at 8, 12 and 16 BeV. The $\gamma n \rightarrow p\pi^-$ cross section is about two to three times the $\gamma p \rightarrow n\pi^+$ cross section. This enhancement is related to the S/V parameter through the equation:

$$\frac{d\sigma}{du}(\pi^{\pm}) = |N|^2 (1 + S/V)^2 + \mathrm{INT}\,(1 + S/V) + |\Delta|^2,$$

where $|N|^2$, INT, $|\Delta|^2$ are the contributions to the cross sections from the nucleon, nucleon-delta interference and Δ respectively. Since S/V = - .376 from our solution and since the INT is positive as it follows from Fig. 3, we expect the π^- cross section to be larger.

At places where the $N\gamma$-trajectory is dominant the prediction that

$$\frac{d\sigma}{du}(\gamma n \to p\pi^-) > \frac{d\sigma}{du}(\gamma p \to n\pi^+)$$

is rather general[13] and it should be checked experimentally.

D. Our solutions at 180^0 extrapolated to low energies pass through the mean of the differential cross sections.

REFERENCES

1. R. Anderson et al., Phys. Rev. Letters 21, 479 (1968).
2. E. A. Paschos, Phys. Rev. Letters 21, 1855 (1968).

   The proposal of this paper is the simplest choice in the absence of the nucleon dip. The new data on $\pi^- p \to p\rho^-$ do not allow such a large $I = 3/2$ contribution. We take this opportunity to correct two misprints which occurred in the final printing of this paper: (i) In Eq. (1) the Γ-function $\Gamma(\alpha-1/2)$ should be replaced by $\Gamma(\alpha+3/2)$. (ii) In Eq. (11), $A_{1/2,1/2}$ should read like (II.5b) in this text.
3. D. Tompkins et al., Phys. Rev. Letters 23, 725 (1969).
4. R. L. Anderson et al., Phys. Rev. Letters 23, 721 (1969).
5. E.W. Anderson et al., Phys. Rev. Letters 22, 102 (1969).
6. J. V. Beaupre, Report No. SLAC-107, UC-34(TH), Stanford Linear Accelerator Center, unpublished.
7. M. Gourdin and Ph. Salin, Nuovo Cimento 27, 193 (1963);
   Ph. Salin, Nuovo Cimento 28, 1294 (1963).
8. G. F. Chew, M. L. Goldberger, F. E. Low and Y. Nambu, Phys. Rev. 106, 1345 (1957).
9. J. S. Ball, Phys. Rev. 124, 2014 (1961).
10. G. Kane, talk presented at the informal meeting on Processes at Backward Angles at SLAC (January 1969).
11. C. B. Chiu and J. D. Stack, Phys. Rev. 153, 1575 (1967).
12. C. C. Shih, Phys. Rev. Letters 22, 105 (1969).
13. V. Barger and P. Weiler, preprint, University of Wisconsin (1969).
14. J. E. Mandula, J. Weyers and G. Zweig, Phys. Rev. Letters 23, 266 (1969);
    V. Barger and C. Michael, Phys. Rev. Letters 22, 1330 (1969).

15. E. A. Paschos, Report No. SLAC-PUB-636, Stanford Linear Accelerator Center (August 1969).

16. Z. G. T. Guiragossián, Report No. SLAC-PUB-657, Stanford Linear Accelerator Center (1969).

TABLE CAPTIONS

1. Comparisons of upper bounds for I=3/2 exchanges with the data and calculated cross sections. The second and third columns give the upper bounds for the contribution of I=3/2 exchanges to the photoproduction cross sections. Columns four and five give the interpolated π^o and π^+ experimental cross sections. Columns six and seven give the percent contribution of the Δ to the calculated cross section.

2. The isotopic spin dependence of the amplitudes. The parameter S/V is the isoscalar to isovector coupling ratio for the I=1/2 exchanges, and is determined by the fit to the data.

TABLE 1

u BeV^2	Upper Bound for π^0 nb/BeV^2	Upper Bound for π^+ nb/BeV^2	$d\sigma/du(\pi^0)$ nb/BeV^2	$d\sigma/du(\pi^+)$ nb/BeV^2	Calculated % Δ to π^0	Calculated % Δ to π^+
E = 8 BeV						
-0.02	5.48	2.74	6.7	5.6	35	18
-0.06	4.56	2.28	6.2	6.3	-	-
-0.13	3.36	1.68	5.0	6.1	69	28
-0.18	2.04	1.02	3.8	5.8	110*	31*
-0.24	1.40	0.70	2.7	4.5	-	32*
-0.32	0.96	0.48	2.2	3.0	126*	32*
E = 16 BeV						
-0.10	0.56	0.28	0.87	-	110*	33
-0.14	0.60	0.30	0.79	0.78	-	41
-0.20	0.48	0.24	0.59	-	154*	43
-0.26	0.36	0.18	0.40	0.61	-	43
-0.33	0.24	0.12	0.27	0.57	184*	44*
-0.43	0.16	0.08	0.22	-	169*	46*
-0.57	0.096	0.048	0.13	-	132*	58*

*The calculated cross section exceeds the bound for these points.

TABLE 2

Reaction	I_α $N_\alpha, N\gamma$	Δ
$\gamma p \rightarrow n\pi^+$	$-\sqrt{2}(1+S/V)$	1
$\gamma p \rightarrow p\pi^0$	$(1-S/V)$	$\sqrt{2}$
$\gamma n \rightarrow p\pi^-$	$-\sqrt{2}(1-S/V)$	1

FIGURE CAPTIONS

1. The fit to π^+ photoproduction. The photon momentum varies somewhat about the indicated average. The theoretical points are calculated using the photon momentum of each point. The data are from Ref. 3.

2. The fit to π^0 photoproduction data of Ref. 4.

3. The percentage contributions of I=1/2 (N_α + $N\gamma$) and I=3/2 (Δ) exchanges to the calculated $\gamma p \rightarrow n\pi^+$ cross section. The $N\gamma$ signature minimum is quite evident near u = -1.2 BeV^2.

4. The predicted cross section for $\gamma n \rightarrow p\pi^-$ at incident photon energies of 8, 12, and 16 BeV.

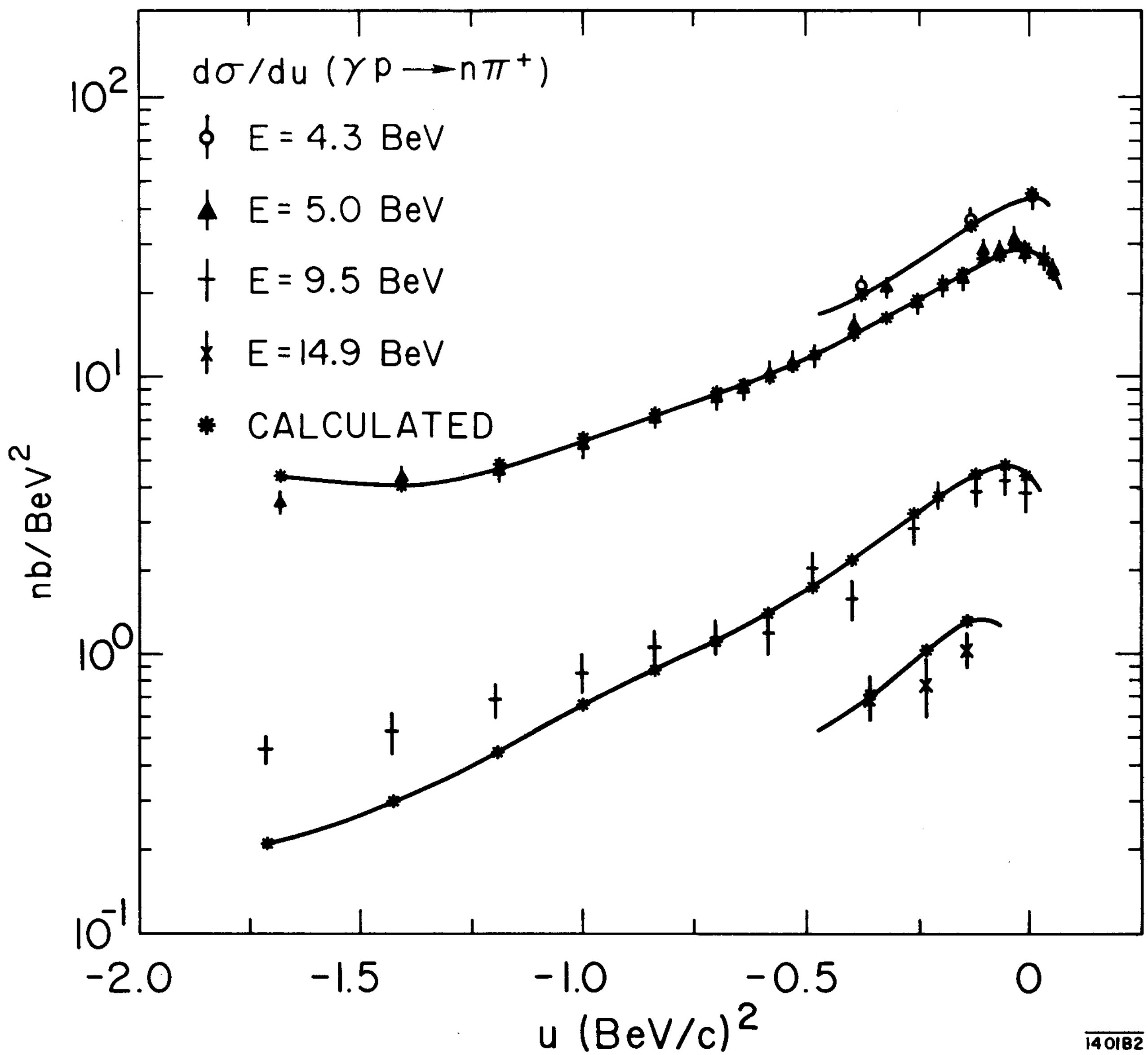

$d\sigma/du\ (\gamma p \longrightarrow n\pi^+)$
E = 4.3 BeV
E = 5.0 BeV
E = 9.5 BeV
E = 14.9 BeV
CALCULATED
10^2
10^1
10^0
10^{-1}
nb/BeV^2
-2.0
-1.5
-1.0
-0.5
0
u (BeV/c)^2
1401B2

Fig. 1

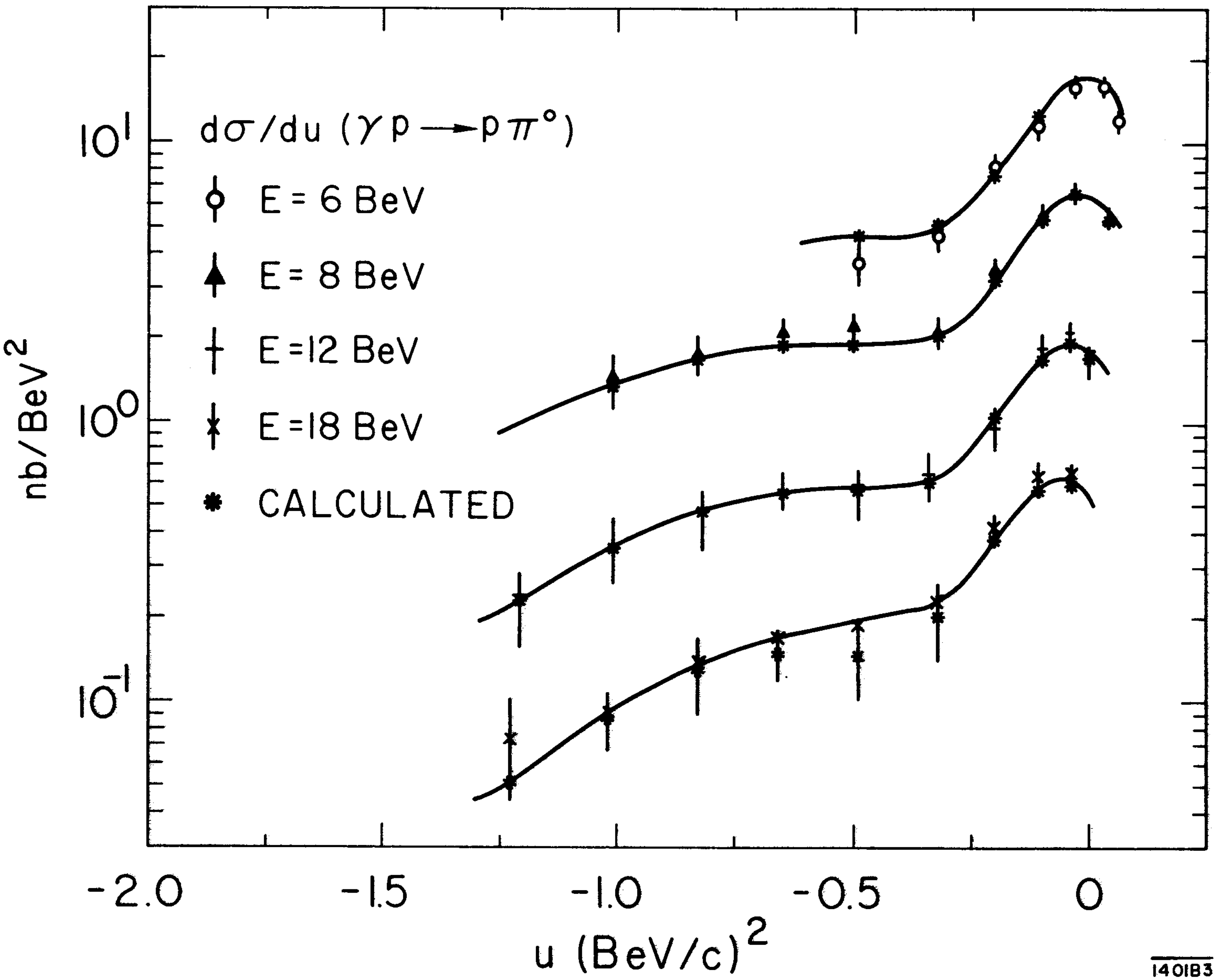

$d\sigma/du\ (\gamma p \longrightarrow p\pi^\circ)$
E = 6 BeV
E = 8 BeV
E = 12 BeV
E = 18 BeV
CALCULATED
10^1
10^0
10^{-1}
nb/BeV^2
-2.0
-1.5
-1.0
-0.5
0
u (BeV/c)^2
1401B3

Fig. 2

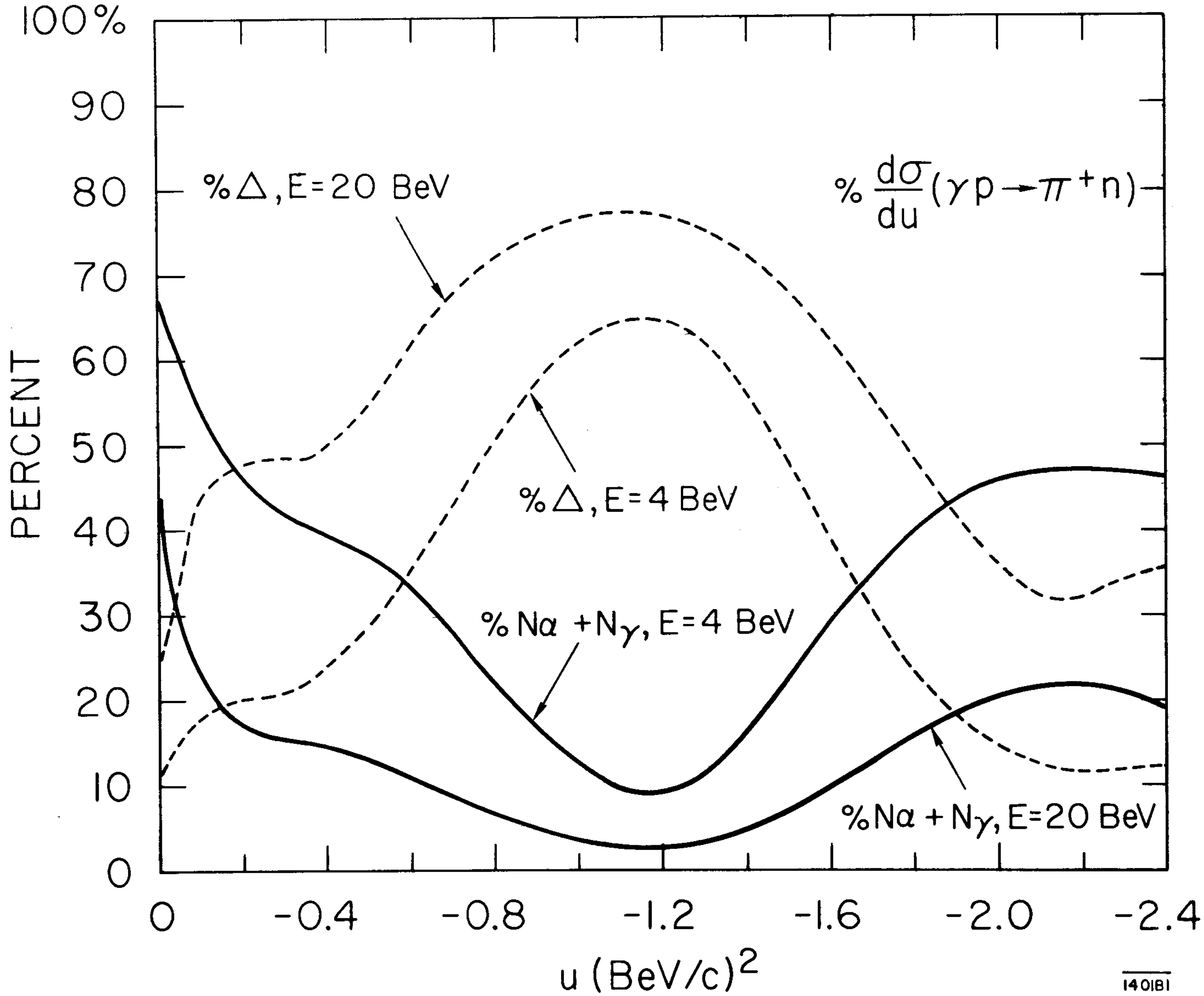
100%
90
80
70
60
50
40
30
20
10
0
PERCENT
0
-0.4
-0.8
-1.2
-1.6
-2.0
-2.4
u (BeV/c)^2
%Δ, E=20 BeV
$\% \frac{d\sigma}{du}(\gamma p \to \pi^+ n)$
%Δ, E=4 BeV
%Nα +Nγ, E=4 BeV
%Nα + Nγ, E=20 BeV
1401B1

Fig. 3

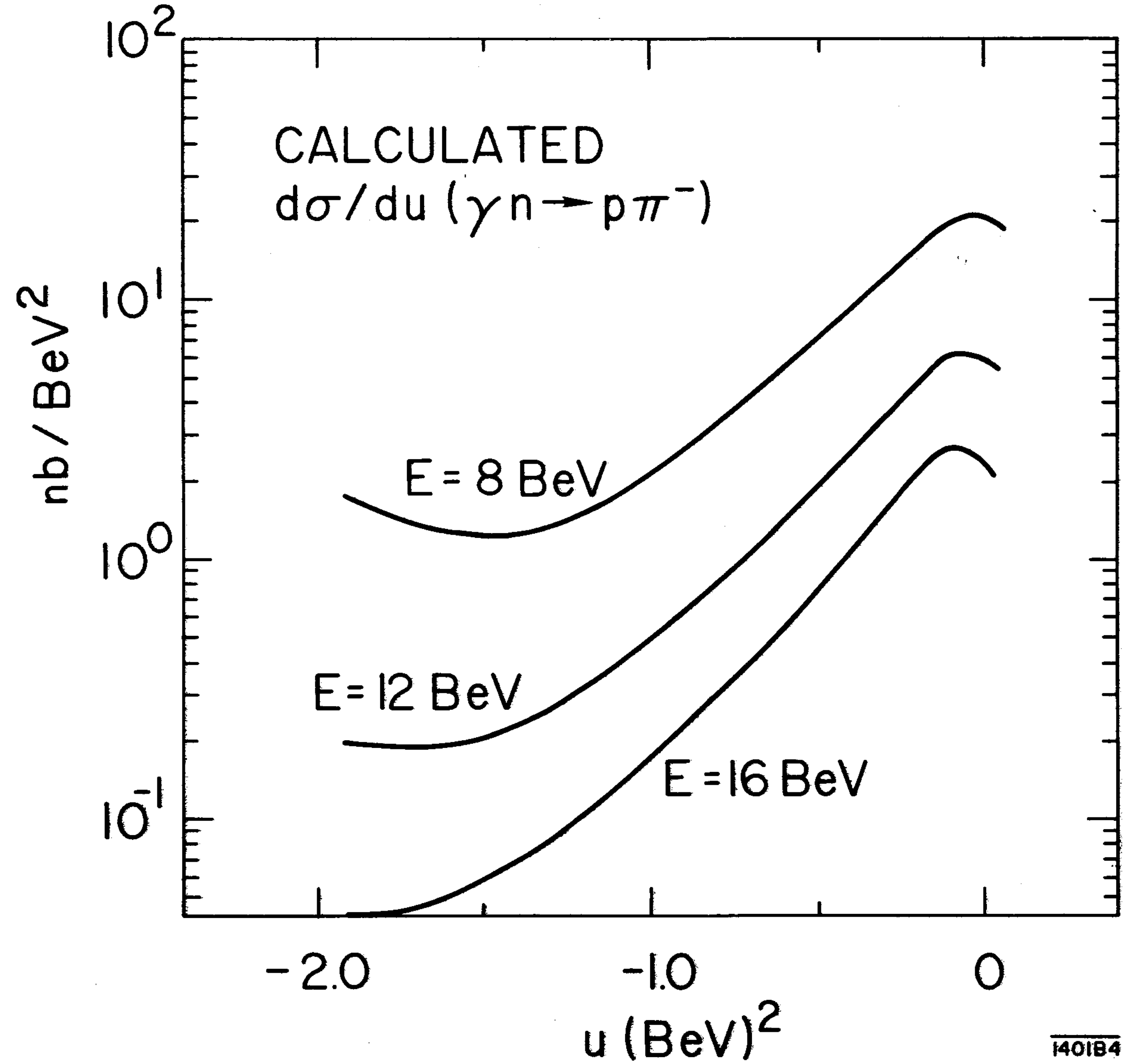

CALCULATED
dσ/du (γn→pπ⁻)
E = 8 BeV
E = 12 BeV
E = 16 BeV
nb / BeV²
u (BeV)²
10²
10¹
10⁰
10⁻¹
-2.0
-1.0
0
1401B4

Fig. 4